Direct and Efficient Optical Coupling Into Plasmonic Integrated Circuits From Optical Fibers

Qian Gao, Fanghui Ren, and Alan X. Wang

***Abstract*— We demonstrate direct and efficient optical coupling from an optical fiber into plasmonic integrated circuits (PICs) at 1.55-μm wavelength using ultra-compact plasmonic dipole nanoantennas. The PICs consist of slot waveguides with single-chip integrated Yagi–Uda antennas. To improve the optical coupling efficiency from optical fibers, we add 500-nm-thick Su-8 film with a high refractive index as the top cladding. We experimentally achieve 8.6% couple-in efficiency from a high numerical aperture fiber to the plasmonic slot waveguide and 46% total couple-out efficiency from the plasmonic slot waveguide. We also quantitatively characterize the dependence of the couple-in efficiency to the spot size of the incident light.**

***Index Terms*— Photonic integrated circuit, surface plasmons, waveguides, antennas.**

I. Introduction

PHOTONIC integrated circuits (PICs) have become the essential solution for chip-to-chip and even on-chip optical interconnects to overcome the bottleneck of electric interconnects of complementary metal–oxide–semiconductor (CMOS) technology. However, there is a size mismatch between nano-sized electronics and micro-sized dielectric PIC components, which is limited by optical diffraction as the fundamental limit to the size scaling of PICs. Plasmonics can bridge the feature size gap between electronics and photonics [1]. Basically, using metallic materials with negative permittivity circumvents the diffraction limit and achieves localization of electromagnetic energy into nanoscale regions [2], [3]. For example, plasmonic slot waveguides based on metal-insulator-metal (MIM) nanostructures are capable of guiding electromagnetic waves with a mode at deep subwavelength scale [4]. Therefore, plasmonic integrated circuits are expected to combine both high operational speeds and ultra-compact footprint rivaling electronics [5], [6]. However, efficient coupling of light into sub-wavelength plasmonic waveguides requires ultra-strong light focusing and excellent mode matching, usually requiring compact silicon waveguides [7]–[9]. Such hybrid integration between plasmonic and dielectric waveguides comes at the difficulty of fabrication, and still requires a large size grating coupler to couple light into the dielectric waveguide first. In the past years, nanocouplers such as plasmonic grating couplers [10]–[12], plasmonic waveguide tapers [13], [14], Luneburg lens [15], nanoantennas [16], [17], and nanoparticle couplers [18], [19] have been implemented to focus and convert light into sub-wavelength plasmonic waveguide mode from free space. Of all those aforementioned nanocouplers, nanoantennas are the most attractive solution and can function simultaneously as a light concentrator and a mode converter with high efficiency [20], [21]. Simulation results show that the coupling efficiency of dipole antennas with side and bottom reflectors can be as high as 26% [22]. Recently, Kriesch et.al reported a total radiation efficiency of $60 \pm 3\%$ from the plasmonic slot waveguide into air and into the substrate using Yagi-Uda nanoantenna [23]. Besides that, bowtie antennas were also investigated as nanocouplers with 10% simulated coupling efficiency of two serially connected bowties antennas [24], [25]. But compared to Yagi-Uda nanoantennas, it has higher absorption loss due to the larger size [26]. However, all these theoretical and experimental results of optical coupling from free space into plasmonic waveguides require high numerical aperture (NA) lenses, which is not convenient for PIC characterization and engineering applications. Direct coupling light from optical fibers into plasmonic integrated circuits using nanoantennas, although extremely pivotal, has not been reported to the best our knowledge.

In this letter, we demonstrate plasmonic integrated circuits based on gold (Au) slot waveguides with on-chip integrated Yagi-Uda nanoantennas, and experimentally implement direct and efficient optical coupling from high NA optical fibers as shown in Fig.1 (a). The plasmonic slot waveguides were fabricated on a 220 nm thick Au film and the whole structure is on top of a 0.5 mm polished quartz substrate with a refractive index of $n_{sub} = 1.44$. The slot width is 300 nm and filled with Su-8, which has a high refractive index of $n_{clad} = 1.565$ at 1.55 μm wavelength. To demonstrate efficient optical coupling, Yagi-Uda nanoantennas are utilized at both ends of the plasmonic slot waveguide. The 500 nm thick high refractive index Su-8 as the top cladding can significantly improve the optical power coupled directly from high NA optical fibers that have focal lengths of only a few microns. We experimentally achieve 8.6% couple-in efficiency and 46% total couple-out efficiency (23% into air and 23% into the substrate). We also quantitatively characterize the couple-in

Manuscript received November 13, 2015; revised January 31, 2016; accepted February 15, 2016. Date of publication February 25, 2016; date of current version April 5, 2016. This work was supported by the National Science Foundation under Grant 1342318 and Grant 1449383.

The authors are with the School of Electrical Engineering and Computer Science, Oregon State University, Corvallis, OR 97331 USA (e-mail: gaoqi@oregonstate.edu; renf@oregonstate.edu; wang@eecs.oregonstate.edu).

Color versions of one or more of the figures in this letter are available online at http://ieeexplore.ieee.org.

Digital Object Identifier 10.1109/LPT.2016.2533583

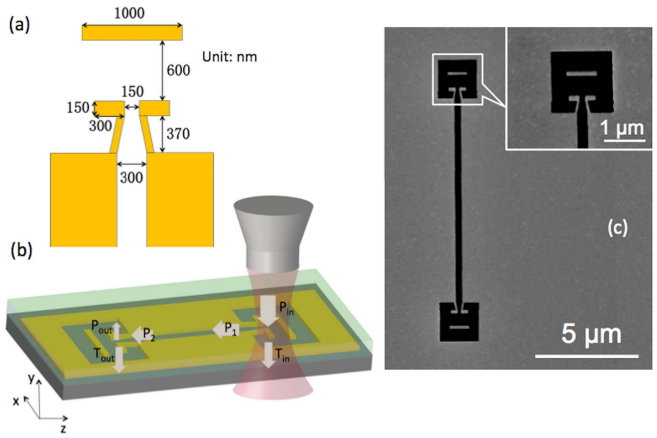

Fig. 1. (a) Top view of dipole nanoantenna; (b) Schematic of optical coupling into plasmonic slot waveguide using dipole antennas from optical fibers; (c) SEM image of the fabricated plasmonic slot waveguide with Yagi-Uda antennas.

efficiency as a function of the spot size of the incident light, and obtain propagation loss of the plasmonic slot waveguide of 0.5 dB/μm.

II. Simulation

Over all, the incident radiation cannot be completely converted into the waveguide mode by the nanoantennas due to Ohmic losses, reflection into air, and direct transmission into the substrate. However, those losses can be minimized by nanoantenna design optimization. Our design of Yagi-Uda nanoantenna uses FullWave™ from Synopsis based on three-dimensional finite-difference time-domain (3-D FDTD) method. At radio frequencies, the character length of the antennas is nearly proportional to the wavelength of incident radiation. At optical frequencies, as a comparison, nanoantennas response to a much longer wavelength, which is called effective wavelength (λ_{eff}). This effective wavelength is determined by the plasmonic wavelength due to the non-negligible penetration depth of the lightwave into metal [26]. The optimized design parameters of the nanoantennas are shown in Fig. 1 (a). The length of the nanoantenna is 300 nm to obtain a resonant wavelength at 1.55 μm. Smaller antenna gap will help to capture more radiation power [27]. Considering the feasibility of our fabrication, the gap width is chosen to be 150 nm. A 370 nm long waveguide taper is used to connect the nanoantenna with the slot waveguide to minimize the impedance mismatch. Furthermore, a 150 nm wide and 1 μm long gold rod is placed 600 nm away in parallel to the dipole antennas, which will reflect the electromagnetic wave constructively back into the dipole antenna to further improve the couple-in efficiency by 2× [22]. By reciprocity invariant theory, a good couple-in antenna is also a good couple-out antenna [27], so the same nanoantenna design is used for both coupling light into the waveguide and coupling out into free space.

In our simulation, a 1.5 μm × 1.5 μm focused Gaussian beam is placed 100 nm above the Yagi-Uda nanoantenna to represent the excitation source from a high NA optical fiber. In our analysis as shown in Fig.1 (b), we define the total incident optical power to be P_{in}, the coupled optical power at

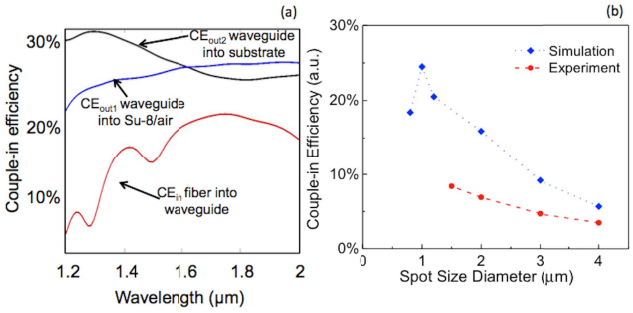

Fig. 2. (a) Simulated optical coupling efficiency as a function of the incident optical wavelength; (b) Simulated couple-in efficiency as a function of the spot diameter.

the end of the input waveguide taper to be P_1. The transmitted power through the nanoantennas into the quartz substrate and the waveguide mode power at the beginning of the output waveguide taper are defined to be T_{in} and P_2 respectively. And the optical power radiated out from the nanoantennas into air and the quartz substrate is expressed to be P_{out} and T_{out}, respectively. The couple-in and couple-out efficiency are defined as:

$$CE_{in} = P_1/P_{in} \times 100\% \quad (1)$$

$$CE_{out1} = T_{out}/P_2 \times 100\% \quad (2)$$

$$CE_{out2} = P_{out}/P_2 \times 100\% \quad (3)$$

Fig. 2 (a) depicts the numerical results of optical coupling efficiency of the Yagi-Uda nanoantenna, CE_{in}, CE_{out1}, and CE_{out2}, as a function of the optical wavelength from 1.2 μm to 2.0 μm. In our design, the couple-in efficiency CE_{in} can achieve 20% and the couple-out efficiency into Su-8/air and the quartz substrate are 26% and 27%. Based on our simulation results, we found that the ratio of the transmitted optical power through the nanoantenna (T_{in}) and the optical power coupled into the slot waveguide (P_1) is 4.4. For the couple-out efficiency, the ratio of T_{out}/P_{out} will remain constant, since this ratio is only determined by the effective refractive indices of the top cladding and the substrate. When the top cladding is 500 nm thick Su-8 in our design, $T_{out}/P_{out} = 1.04$, which is much more uniform than $T_{out}/P_{out} = 2$ in Ref [23]. Based on reciprocity invariant theory, CE_{in} should equal to CE_{out2} at all wavelength. However, due to the mismatch of the radiation profile from the Yagi-Uda antenna and the incident light from the high NA fiber, the actual couple-in efficiency is lower than the couple-out efficiency. We further investigate the dependence of the couple-in efficiency on the spot size of the incident beam as shown in Fig.2 (b). The optimal incident beam diameter is 1 μm. Increase of the incident beam size will decrease the couple-in efficiency as a smaller fraction of the incident power can be captured by the limited size of the nanoantennas. Interestingly, by further reducing the beam size (<1 μm), the couple-in efficiency decreases rapidly as well. This is because the divergent angle of the incident beam becomes very big due to the diffraction limit, which exceeds the acceptance angle of the Yagi-Uda nanoantenna.

Fig.3 (a) depicts the simulated optical power profile at the symmetric plane along the slot waveguide at 1.55 μm

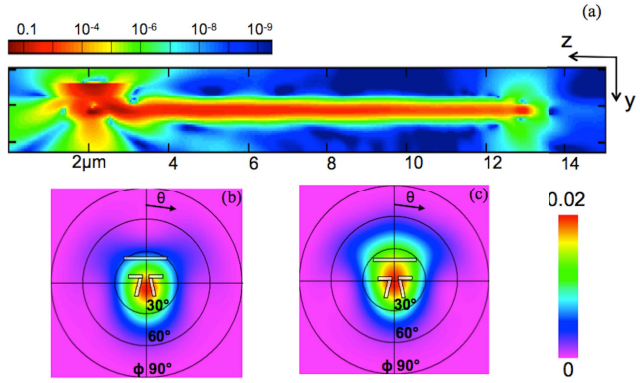

Fig. 3. (a) 3-D FDTD simulation of the optical power profile along waveguide; far field radiation pattern into (b) the quartz substrate and into (c) Su8/air.

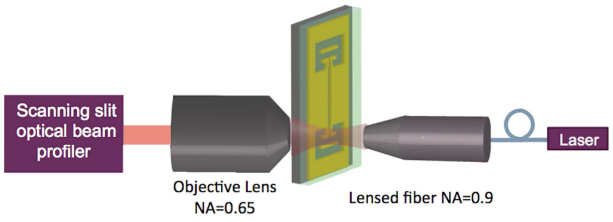

Fig. 4. Configuration of the experimental setup used for coupling efficiency measurement.

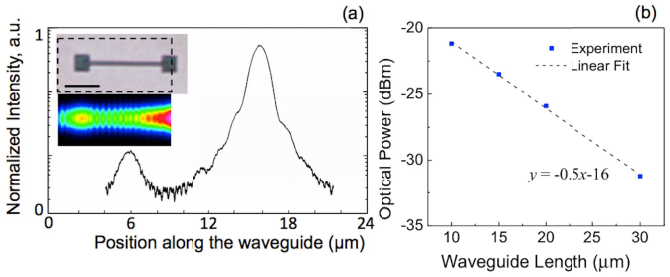

Fig. 5. (a) Optical intensity profile in log scale of plasmonic slot waveguide with Yagi-Uda antennas, and the insert figures show the optical image of the device and the near field image of the 10 μm waveguide, scale bar is 5 μm; (b) Measured output power for plasmonic slot waveguides with different lengths.

incident wavelength. We can clearly see the reflected, scattered, transmitted, and coupled power at the receiving antenna. Along the plasmonic slot waveguide, the optical power is well confined. At the transmitting antenna, the optical power radiates out into Su-8/air and the quartz substrate in surface normal directions with slight scattering. The far field radiation patterns into the quartz substrate and air are also presented in Fig. 3 (b) and (c). The designed Yagi-Uda nanoantenna emits light with strong directionality within a polar cone of 30°, which is sufficiently narrow that can be effectively collected by a high NA optical fiber. Compared with Ref [23], adding a thin layer high index top cladding significantly improves the symmetry of the far field emission patterns.

III. Experiment

We started the fabrication processes by cleaning a 1"×1" 500 μm thick polished quartz substrate with acetone, isopropyl alcohol, and de-ionized water. A 220 nm gold thin film was deposited by thermal evaporation with a deposition rate at 5 Å/s. The device was than patterned by a 30 KV focused-ion beam (FIB) (Quanta 3D, FEI Company) lithography system with slot width of 300 ± 10 nm. To minimize the background signal, the receiving (couple-in) and transmitting (couple-out) antennas were patterned within a $1.5\mu\text{m} \times 1.5\mu\text{m}$ window as shown in Fig.1 (c). Following the FIB process, Su-8 was spin-coated and then hard baked for 20 min at 200 °C to form a 500 nm thick top cladding. Waveguides with different lengths (L = 10 μm, 15 μm, 20 μm and 30 μm) were fabricated using same receiving and transmitting antennas. The scanning electron microscopy (SEM) image in Fig. 1(c) depicts the fabricated 10 μm plasmonic slot waveguide with the zoomed view of the Yagi-Uda nanoantenna.

The optical characterization system is shown in Fig.4. The sample was mounted on a three-dimensional translation/rotation stage, allowing highly precise angular adjustment and spatial alignment regarding to the incident light spot. Light from a 1.55 μm laser was coupled into a single-mode polarization-maintaining (PM) fiber with high numerical aperture (NA) of 0.9 (PROFA™ 1-D from Chiral Photonics, Inc.). It utilizes a "vanishing core" concept to achieve such high NA [28]. The high NA fiber is capable of focusing the beam spot to a minimum size of 2 μm × 2 μm and can be precisely aligned to the receiving nanoantenna through monitoring the output power from the transmitting antenna. The incident radiation is polarized along the antenna arms, designated as the transverse electric (TM) to the plasmonic slot waveguide. All the transmitted light ($T_{out} + T_{in}$) is collected by an objective lens with NA = 0.65 on the other side of sample, and was then monitored by an optical beam profiler.

Fig.5 (a) presents the measured intensity profile along the 10 μm plasmonic slot waveguide. The higher peak represents the direct transmitted incident light (T_{in}) and the lower one denotes the light radiated into the substrate (T_{out}), and the light between these two peaks come from the optical scattering of the slot waveguide. The optical power of T_{in} and T_{out} can be obtained by integration of the intensity data from the beam profiler along the waveguide. The total incident power P_{in} from the high NA fiber can be measured by the transmitted light through the open window without an antenna (1.5 μm × 1.5 μm), which is −7.7 dBm. For the 10 μm waveguide, the measured T_{in} is −11.96 dBm and T_{out} is −21.19 dBm. After measuring the T_{out} from all of these waveguides with different lengths, we plotted the data in Fig. 5 (b) with a linear fitting curve. The propagation loss, which is the slope of the linear fitting curve, is determined to be 0.5 dB/μm, which is higher than the simulation result of 0.3 dB/μm. This is possibly due to FIB lithography induced roughness on sidewalls of the slot and higher Ohm losses of thin gold film than the ideal permittivity. The couple-in and couple-out efficiencies can be calculated by utilizing the ratio of $T_{in}/P_1 = 4.4$ and $T_{out}/P_{out} = 1$ from simulation, which are 8.6% and 46% total couple-out efficiency (23% to air and 23% to the substrate) in average. In order to further increase

the optical coupling efficiency, we may follow the approach as pointed out in Ref [23] to reduce the gap width of the plasmonic nanoantennas in our future work.

To characterize the dependence of the couple-in efficiency with the incident beam spot, we vary the size of the incident beam spot. Since the light from the high NA fiber is highly divergent, the incident beam spot size can be enlarged by moving the fiber away and then measured by the optical beam profiler. The minimum beam spot size from the high NA fiber is 2 μm. However, with the confinement of the optical window, we can normalize the incident beam spot to 1.5 μm. We measured T_{out} with different incident spot diameters of 1.5 μm, 2 μm, 3 μm and 4 μm, and the experimentally measured data of the couple-in efficiency is plotted in Fig. 2 (b). The overall trend matches the simulation results very well. However, the lower experimental couple-in efficiencies compared to the simulation results possibly comes from 1) the optical loss of the thermally evaporated gold film is much larger than the perfect gold film used in the simulation [29]; 2) the surface-roughness and other fabrication imperfection of the plasmonic nanoantennas; 3) the slight misalignment in the optical characterization.

IV. Conclusion

In conclusion, we have demonstrated direct and efficient optical coupling into plasmonic integrated circuit from high NA optical fibers using ultra-compact and low loss dipole nanoantennas. To achieve high optical coupling efficiency, we add a 500 nm thick Su-8 film with a high refractive index as the top cladding, which can significantly improve the optical coupling efficiency from optical fibers. We experimentally achieve 8.6% couple-in efficiency from the high NA fiber to the plasmonic slot waveguide, 46% total couple-out efficiency from the plasmonic slot waveguide to air and the substrate, and quantitatively characterize the dependence of the couple-in efficiency to the spot size of the incident light. Such ultra-compact plasmonic slot waveguides with single-chip integrated dipole nanoantennas can play crucial roles for future PICs.

References

[1] R. Zia, J. A. Schuller, A. Chandran, and M. L. Brongersma, "Plasmonics: The next chip-scale technology," *Mater. Today*, vol. 9, nos. 7–8, pp. 20–27, Jul./Aug. 2006.

[2] K. C. Y. Huang, M.-K. Seo, T. Sarmiento, Y. Huo, J. S. Harris, and M. L. Brongersma, "Electrically driven subwavelength optical nanocircuits," *Nature Photon.*, vol. 8, no. 3, pp. 244–249, Feb. 2014.

[3] D. K. Gramotnev and S. I. Bozhevolnyi, "Plasmonics beyond the diffraction limit," *Nature Photon.*, vol. 4, no. 2, pp. 83–91, Jan. 2010.

[4] G. Veronis and S. Fan, "Modes of subwavelength plasmonic slot waveguides," *J. Lightw. Technol.*, vol. 25, no. 9, pp. 2511–2521, Sep. 2007.

[5] V. J. Sorger, R. F. Oulton, R.-M. Ma, and X. Zhang, "Toward integrated plasmonic circuits," *MRS Bull.*, vol. 37, no. 8, pp. 728–738, Aug. 2012.

[6] A. Melikyan *et al.*, "Plasmonic-organic hybrid (POH) modulators for OOK and BPSK signaling at 40 Gbit/s," *Opt. Exp.*, vol. 23, no. 8, pp. 9938–9946, Apr. 2015.

[7] C. Delacour *et al.*, "Efficient directional coupling between silicon and copper plasmonic nanoslot waveguides: Toward metal–oxide–silicon nanophotonics," *Nano Lett.*, vol. 10, no. 8, pp. 2922–2926, Jul. 2010.

[8] R. M. Briggs, J. Grandidier, S. P. Burgos, E. Feigenbaum, and H. A. Atwater, "Efficient coupling between dielectric-loaded plasmonic and silicon photonic waveguides," *Nano Lett.*, vol. 10, no. 12, pp. 4851–4857, Oct. 2010.

[9] A. Melikyan, M. Kohl, M. Sommer, C. Koos, W. Freude, and J. Leuthold, "Photonic-to-plasmonic mode converter," *Opt. Lett.*, vol. 39, no. 12, pp. 3488–3491, Jun. 2014.

[10] T. Aihara *et al.*, "Coherent plasmonic interconnection in silicon-based electrical circuit," *J. Lightw. Technol.*, vol. 33, no. 10, pp. 2139–2145, May 15, 2015.

[11] C. Ropers, C. C. Neacsu, T. Elsaesser, M. Albrecht, M. B. Raschke, and C. Lienau, "Grating-coupling of surface plasmons onto metallic tips: A nanoconfined light source," *Nano Lett.*, vol. 7, no. 9, pp. 2784–2788, Aug. 2007.

[12] M. G. Nielsen and S. I. Bozhevolnyi, "Highly confined gap surface plasmon modes in metal strip–gap–film configurations," *J. Opt. Soc. Amer. B*, vol. 32, no. 3, pp. 462–467, Mar. 2015.

[13] E. Feigenbaum and M. Orenstein, "Backward propagating slow light in inverted plasmonic taper," *Opt. Exp.*, vol. 17, no. 4, pp. 2465–2469, Feb. 2009.

[14] Y. Song, J. Wang, Q. Li, M. Yan, and M. Qiu, "Broadband coupler between silicon waveguide and hybrid plasmonic waveguide," *Opt. Exp.*, vol. 18, no. 12, pp. 13173–13179, Jun. 2010.

[15] B. Arigong *et al.*, "Design of wide-angle broadband luneburg lens based optical couplers for plasmonic slot nano-waveguides," *J. Appl. Phys.*, vol. 114, no. 14, p. 144301, Oct. 2013.

[16] A. Andryieuski, V. A. Zenin, R. Malureanu, V. S. Volkov, S. I. Bozhevolnyi, and A. V. Lavrinenko, "Direct characterization of plasmonic slot waveguides and nanocouplers," *Nano Lett.*, vol. 14, no. 7, pp. 3925–3929, Jun. 2014.

[17] F. Obelleiro, J. M. Taboada, D. M. Solís, and L. Bote, "Directive antenna nanocoupler to plasmonic gap waveguides," *Opt. Lett.*, vol. 38, no. 10, pp. 1630–1632, May 2013.

[18] S. Zhang, C. Gu, and H. Xu, "Single nanoparticle couplers for plasmonic waveguides," *Small*, vol. 10, no. 21, pp. 4264–4269, Jul. 2014.

[19] R. Frank, "Coherent control of floquet-mode dressed plasmon polaritons," *Phys. Rev. B*, vol. 85, no. 19, p. 195463, May 2012.

[20] J.-S. Huang, T. Feichtner, P. Biagioni, and B. Hecht, "Impedance matching and emission properties of nanoantennas in an optical nanocircuit," *Nano Lett.*, vol. 9, no. 5, pp. 1897–1902, Apr. 2009.

[21] L. Novotny and N. van Hulst, "Antennas for light," *Nature Photon.*, vol. 5, no. 2, pp. 83–90, Feb. 2011.

[22] A. Andryieuski, R. Malureanu, G. Biagi, T. Holmgaard, and A. Lavrinenko, "Compact dipole nanoantenna coupler to plasmonic slot waveguide," *Opt. Lett.*, vol. 37, no. 6, pp. 1124–1126, Mar. 2012.

[23] A. Kriesch, S. P. Burgos, D. Ploss, H. Pfeifer, H. A. Atwater, and U. Peschel, "Functional plasmonic nanocircuits with low insertion and propagation losses," *Nano Lett.*, vol. 13, no. 9, pp. 4539–4545, Aug. 2013.

[24] A. Andryieuski, R. Malureanu, J. Bouillard, A. V. Zayats, and A. V. Lavrinenko, "Improving plasmonic waveguides coupling efficiency using nanoantennas," in *Proc. IEEE 14th Int. Conf. Transparent Opt. Netw. (ICTON)*, Jul. 2012, pp. 1–4.

[25] C. A. Balanis, *Antenna Theory: Analysis and Design*. Hoboken, NJ, USA: Wiley. 1997.

[26] L. Novotny, "Effective wavelength scaling for optical antennas," *Phys. Rev. Lett.*, vol. 98, no. 26, p. 266802, Jun. 2007.

[27] A. E. Krasnok *et al.*, "Optical nanoantennas," *Phys.-Usp.*, vol. 56, no. 6, p. 539, Jun. 2013.

[28] V. I. Kopp, J. Park, M. Wlodawski, J. Singer, D. Neugroschl, and A. Z. Genack, "Chiral fibers: Microformed optical waveguides for polarization control, sensing, coupling, amplification, and switching," *J. Lightw. Technol.*, vol. 32, no. 4, pp. 605–613, Feb. 15, 2014.

[29] F. Ren, X. Wang, and A. X. Wang, "Thermo-optic modulation of plasmonic bandgap on metallic photonic crystal slab," *Appl. Phys. Lett.*, vol. 102, no. 18, p. 181101, May 2013.